Virchows Arch [Cell Pathol] (1985) 48:33–45

Virchows Archiv B

Mucopolysaccharidosis-like alterations in cardiac valves of rats treated with tilorone

Gerhard Horstmann and Renate Lüllmann-Rauch
Anatomisches Institut der Universität Kiel, Olshausenstraße 40–60, D-2300 Kiel, Federal Republic of Germany

Summary. The purpose of this study was to examine whether the aortic and mitral valves of rats are involved in the mucopolysaccharidosis-like disorder induced by tilorone. Rats were treated with large doses of the drug for periods of 1–21 weeks. After chronic drug treatment the leaflets of both heart valves were thickened and opaque. In all treated animals the spongiosa layer of the stroma was crowded with vacuolated cells; the fibrosa layer was altered only after prolonged treatment. Ultrastructurally, the vacuolated cells of the spongiosa could be identified as histiocytes and fibroblasts, the former being the most susceptible cell type. The fibroblasts of the fibrosa represented the least sensitive cell type. The histochemical results showed that the clear cytoplasmic vacuoles in the spongiosa cells were due to lysosomal storage of polyanionic material with staining characteristics similar to cartilage matrix. After discontinuation of drug treatment the alterations persisted for several weeks. The present study shows that heart valves are involved in the mucopolysaccharidosis-like disorder induced by tilorone. The molecular pathomechanism of the disorder and the exact identification of the storage material must await further analysis.

Key words: Cardiac valves – Lysosomal storage – Acid glycosaminoglycans – Tilorone – Rat

Introduction

Tilorone, a compound which stimulates interferon production and has antiviral and anti-tumor activities (Regelson 1981), has been observed previously in rats to cause lysosomal storage of polar lipids or of acid glycosaminoglycans (aGAG) depending on the cell type (Lüllmann-Rauch 1982, 1983). For example, in hepatocytes lipidosis was prominent, while splenic and

Offprint requests to: R. Lüllmann-Rauch at the above address

hepatic sinus endothelia displayed the cytological features of mucopolysaccharidosis. The latter diagnosis was based on the histochemical and cytochemical demonstration of highly polyanionic storage material, which was water-soluble and not fixable by routine methods used for electron microscopy. The diagnosis of mucopolysaccharidosis was further supported by preliminary findings showing increased urinary excretion of hexuronic acids.

While the molecular pathogenesis of the tilorone-induced aGAG storage is still unknown, the resulting cytological picture is closely reminiscent of that seen in inherited mucopolysaccharidoses. Thus the question arose whether tilorone-induced aGAG-storage also resembles the inherited storage diseases with respect to the organ pattern. We have therefore undertaken a series of investigations focussed on those organs or tissues that are known to be prominently affected in inherited mucopolysaccharidoses (Spranger 1972; Van Hoof 1973). This paper deals with alterations in cardiac valves of the rat; corresponding changes in the cornea and cartilage will be described elsewhere.

Material and methods

1. Materials. Young male and female Wistar rats with an initial body weight of approximately 40 g were used. Tilorone-HCl was a gift of Merrell Dow Pharmaceuticals (Cincinnati, Ohio, USA). For the histochemical investigations the following chemicals were used: Toluidine blue O, $FeCl_3 \cdot 6\,H_2O$ and $MgCl_2 \cdot 6\,H_2O$ (Merck, Darmstadt, FRG); Alcian blue 8 GX (Gurr, Hopkin & Williams, Chadwell Heath, GB); N,N-dimethyl-m-phenylenediamine, N,N-dimethyl-p-phenylenediamine, and trimetaphosphate (Sigma, München, FRG).

2. Animal experiments. Two series of experiments were performed: group I for subchronic drug treatment (up to 7 weeks), group II for chronic drug treatment (up to 5 months). In group I 22 rats of either sex received a daily intraperitoneal injection of tilorone-HCl (50 mg/kg of body weight) for 3–7 weeks. The drug was dissolved in 0.9% NaCl and was given in a volume of 2 ml/100 g body weight. Four of the rats were allowed to survive without further tilorone treatment for 2 and 4 weeks, respectively, after a treatment period of 6 weeks. For some histochemical experiments, additional rats were treated orally for 1.5 to 3 weeks; the drug was either given by stomach tube (100 mg/kg) or mixed with the food as described below. In group II 8 female rats were treated orally with tilorone for 11, 12, 13, 15 and 21 weeks, respectively. The drug was added to the ground food at a concentration of 0.1% resulting in a daily drug uptake of 60–90 mg/kg. Three of these rats, treated for 13 weeks, were allowed to survive without drug administration for further 4, 7 and 15 weeks, respectively. In each group, age-matched control rats were kept under identical conditions without receiving tilorone.

3. Routine morphology. At the end of the experiments the animals were deeply anaesthetized with pentobarbital and killed by vascular perfusion with 3% glutaraldehyde (in 0.1 M phosphate buffer; or in 0.1 M cacodylate buffer plus 3% sucrose; pH 7.2). For perfusion, a cannula was inserted into the left ventricle; the right atrium was opened to release the perfusate. After perfusion, the left ventricle was opened along its outflow tract and the aortic and mitral valves were photographed in situ. The three cusps of the aortic valve were removed individually, each attached to a 2 mm piece of the ascending aorta. In addition, the posterior cusp of the mitral valve was removed. Tissues were postfixed with unbuffered 2% OsO_4, dehydrated with ethanol and embedded in Araldite. Semithin sections (1 μm) were stained with toluidine blue-pyronin (Ito and Winchester 1963). Ultrathin sections were stained with acetate and lead citrate and viewed with Zeiss EM 9 or Philips E 300 electron microscope.

4. Histochemistry. For all histochemical procedures the cusps of the glutaraldehyde-fixed valves were used as whole mounts. For identification of lysosomal organelles, the cytochemical demonstration of trimetaphosphatase was performed according to Doty et al. (1977).

In order to characterize the lysosomal storage material, three methods were employed as previously described in detail (Lüllmann-Rauch 1982).

(a) *Staining with Toluidine blue.* Glutaraldehyde-fixed cusps were incubated for 5 min in 0.1% toluidine blue at pH 2 or pH 5 (Michaelis-buffer), rinsed (5 min) in the corresponding buffer, dehydrated with ethanol, cleared with xylene and mounted in DePeX for light microscopic examination. Mast cells regularly present in the connective tissue at the base of the cusps served as reference for evaluation of the staining results.

(b) *Staining with Alcian blue and determination of the "critical electrolyte concentration" according to Scott and Dorling (1965).* Glutaraldehyde-fixed cusps were incubated for 20 h in 0.05% Alcian blue (in 0.025 M acetate buffer, pH 5.8) containing various $MgCl_2$ concentrations (from 0.2 to 0.7 M). Small pieces of the tracheal wall containing cartilage and mast cells were included in each staining experiment and served as a reference. After incubation the tissues were briefly rinsed in buffer containing the corresponding $MgCl_2$ concentration, dehydrated and mounted in DePeX for light microscopic examination.

(c) *"High-iron-diamine" method (HID).* Fixed cusps were incubated for 20 h in a medium described by Spicer et al. (1978). For a positive control, colonic glands were treated in the same way, and for a negative control, cusps were incubated in a medium where $FeCl_3$ was replaced by $MgCl_2$. Ultrathin sections were examined unstained.

5. Endocytosis experiment

One rat, treated orally with tilorone for 21 weeks, and an age-matched control rat received a single intravenous injection of iron dextran (Myofer 100, Hoechst, Frankfurt, FRG) 24 h before sacrifice, at a dose corresponding to 10 mg Fe/100 g body weight. The aortic valve was fixed and embedded in Araldite. For light microscopy, semithin sections were stained with Turnbull's blue and Safranin after removal of the Araldite with NaOH-ethanol. Ultrathin sections were examined unstained.

Results

1. Gross examination

After subchronic drug treatment (group I), the leaflets of the aortic and mitral valves appeared less transparent than those of controls. After chronic treatment (group II) the leaflets were opaque and thickened (Fig. 1); this was most conspicuous at the nodules and at the lines of closure. The chordae tendineae were also thickened.

2. Light and electron microscopy

Control animals. The structure of control valves was essentially similar to the descriptions in the literature (Pfuhl 1929; Gross and Kugel 1931; Gross 1961; v. Albertini 1953; Kühnel 1966). The two principal layers of the stroma, the spongiosa and fibrosa, could be distinguished (Fig. 2); the spongiosa contained histiocytes as the principal cell type and a few fibroblasts, while the fibrosa harboured fibroblasts only. The histiocytes could be distinguished from fibroblasts of the spongiosa by a coarser heterochromatin

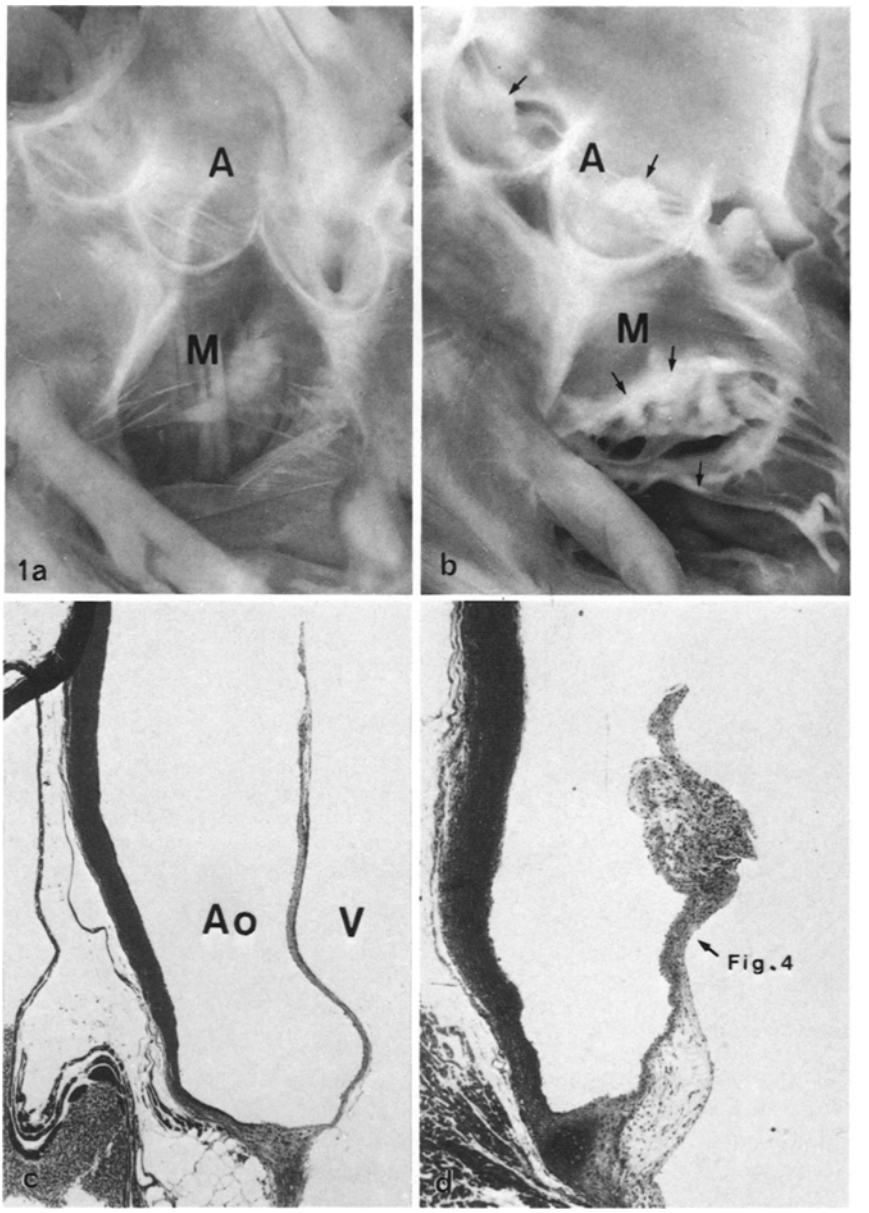

Fig. 1. Left heart valves of a control rat (**a, c**) and a rat chronically treated (**b, d**) with tilorone (15 wk, 85 mg/kg p.o.). Both animals were 18 weeks of age. **a, b** The left ventricles are cut along the outflow tract and the aortic and mitral valves are exposed. In the control, the valvular cusps are transparent; in the treated rat the cusps are opaque and thickenings are seen at the noduli Arantii, at the lines of closure and at the chordae tendineae (*arrows*). ×10. **c, d** Aortic valves in semithin sections. The cusp of the treated rat displays irregular thickenings. The marked region is shown in Fig. 4 at higher magnification. Toluidine blue-pyronin. ×25

Abbreviations used throughout the figures: *A* aortic valve; *Ao* aortic surface of the aortic cusp; *Atr* atrial surface of the mitral leaflet; *E* endothelium; *F* fibrosa layer; *Fb* fibroblast; *H* histiocyte; *M* mitral valve; *N* nucleus; *S* spongiosa layer; *V* left ventricle, or ventricular surface of the aortic or mitral cusps

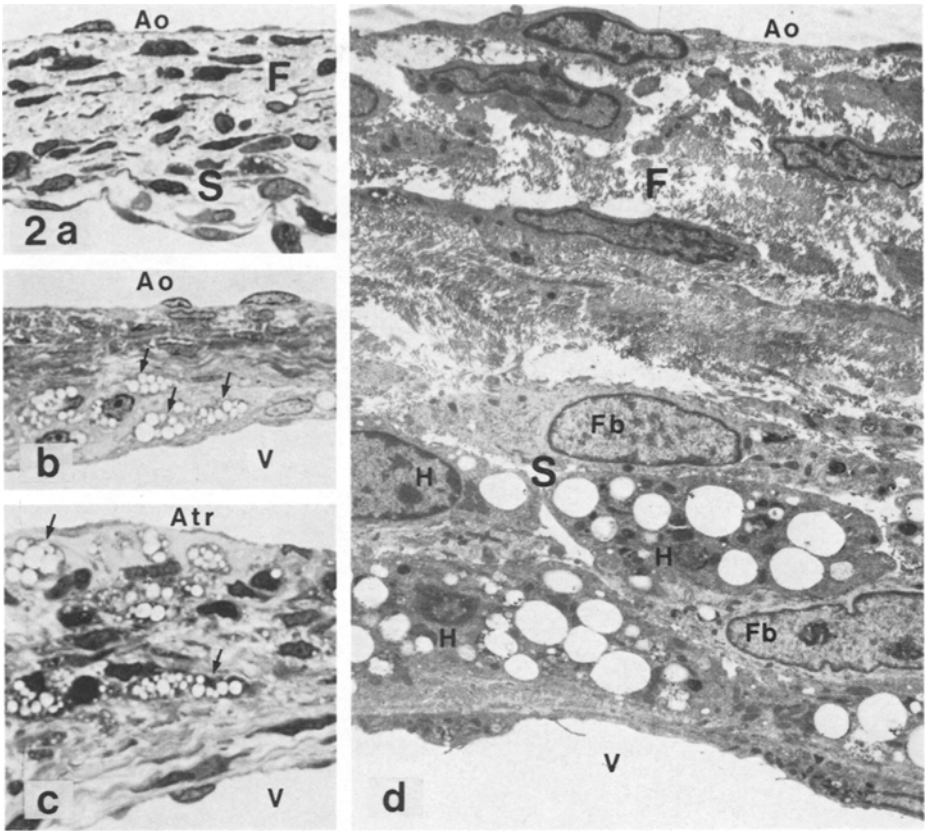

Fig. 2. **a** Aortic cusp of a control rat. The fibrosa and spongiosa layers can be distinguished. **b** Aortic cusp of a rat subchronically treated with tilorone (4 wk, 50 mg/kg i.p.). Vacuolated cells (*arrows*) are seen in the spongiosa layer facing the ventricular lumen. **c** Mitral cusp of a rat subchronically treated with tilorone (7 wk, 50 mg/kg i.p.). Vacuolated cells (*arrows*) are seen in the spongiosa layer facing the atrial lumen. **a**, **b**, **c** semithin sections, toluidine blue-pyronin, ×720. **d** Electron micrograph of the same aortic cusp as in **b**. Numerous empty vacuoles are seen in the histiocytes, whereas the fibroblasts of the spongiosa show few vacuoles only. The fibroblasts of the fibrosa are even less altered. ×4,000. For abbreviations, see legend to Fig. 1

structure, a more electron-dense cytoplasm, numerous endocytic vesicles, some small empty vacuoles and by high avidity to ingest intravenously injected iron dextran. The fibroblasts, on the other hand, were characterized by a less electron-dense cytoplasm and an elaborated rough endoplasmic reticulum.

Treated animals. Group I. Initially, the most prominent pathological feature, observed in both heart valves, was cytoplasmic vacuolation of the cells in the spongiosa layer (Fig. 2). Ultrastructurally (Fig. 3), most of the severely vacuolated cells could be identified as histiocytes. The cytoplasmic vacuoles varied greatly in size (0.5–5 μm); they were membrane-limited and appeared

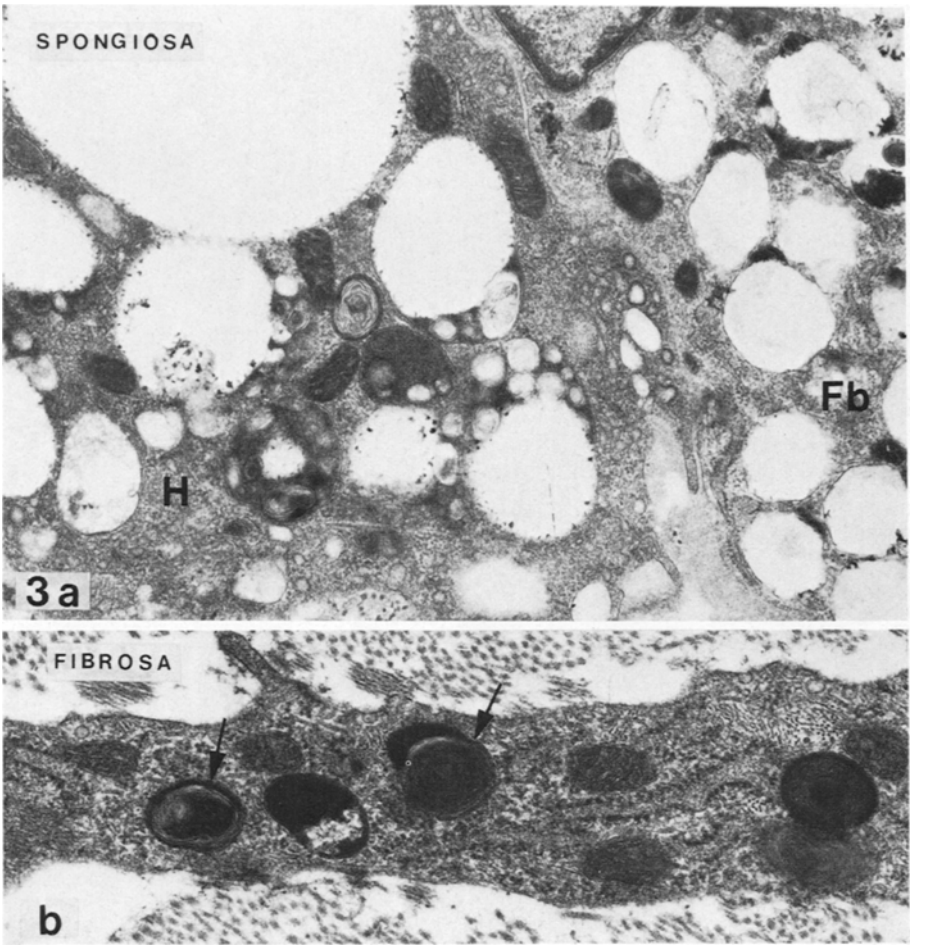

Fig. 3. a Histiocyte and fibroblast in the spongiosa layer of the same mitral cusp as in Fig. 2**c** (tilorone 7 wk). Clear vacuoles are seen in both cells. × 18,500. **b** Fibroblast in the fibrosa layer of the same aortic cusp as in Figs. 2**b**, **d**. *Arrows* point to lamellated inclusions. × 34,000. For abbreviations, see legend to Fig. 1

largely empty, except for remnants of an electron-dense matrix adherent to the limiting membrane. In addition, single lamellated inclusions were seen in the histiocytes, or lamellated structures were found embedded in the electron-dense matrix of the vacuoles. When the drug treatment was continued for more than 4 weeks, most fibroblasts of the spongiosa layer (Fig. 3a) also showed membrane-limited vacuoles which were smaller (0.5–1 μm) and more homogeneous in size than those in histiocytes. Often, the vacuoles of the spongiosa fibroblasts contained small amounts of flocculent electron-lucent material. Remarkably, the fibroblasts of the fibrosa layer were much less affected (Fig. 3b); they usually displayed a few vacuoles and lamellated inclusion bodies.

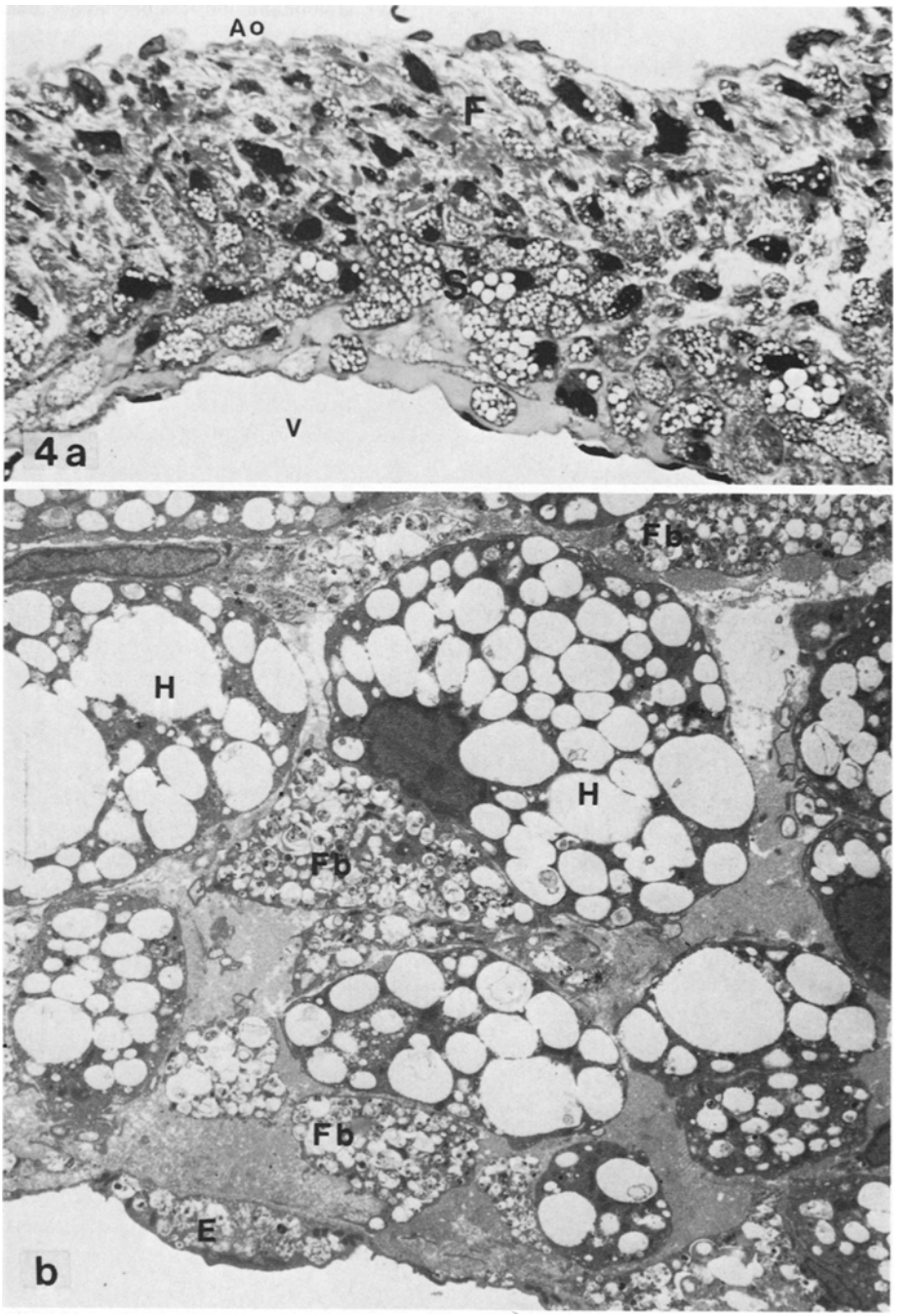

Fig. 4a, b. Aortic cusp of the same valve as shown in Figs. 1**b**, **d** (tilorone 15 wk). **a** In the semithin section, the spongiosa is seen to be crowded with vacuolated cells; the fibrosa cells also show clear vacuoles. Toluidine blue-pyronin, ×640. **b** Low power electron micrograph of the spongiosa. The histiocytes are greatly swollen due to vacuolation. The fibroblasts show numerous small vacuoles and polymorphous inclusions; similar inclusions are seen in the endothelial cells. ×4,000. For abbreviations, see legend to Fig. 1

Group II. After chronic drug treatment (Fig. 4), the spongiosa layers in both heart valves were filled with vacuolated histiocytes and fibroblasts; the fibroblasts of the fibrosa layer also showed clear vacuoles. In addition, fibroblasts with morphological signs of degeneration occurred in both stromal layers; such cells (Fig. 4b) were filled with polymorphous inclusions and vacuoles, many of which resembled autophagic vacuoles. The macroscopic thickenings seen at the lines of closure and at the nodules (Fig. 1) were mainly due to accumulations of vacuolated cells.

Histiocytes and fibroblasts with numerous clear vacuoles were regularly observed also in the cardiac skeleton and subendocardium and in the interstitial tissue of myocardium. In the endothelial cells covering the valvular leaflets, single vacuoles with flocculent material were observed after subchronic drug treatment, and numerous vacuoles of the same type were found after chronic treatment (Fig. 4b).

3. Enzyme histochemistry

After 3 weeks of tilorone treatment, trimetaphosphatase (Doty et al. 1977) was most readily demonstrated in the vacuolated cells of the spongiosa (Fig. 5a). Ultrastructurally (Fig. 5b), the precipitates were found in the tilorone-induced vacuoles and lamellated inclusions of histiocytes.

4. Endocytosis experiment

Iron dextran was injected intravenously as a tracer which is known to be phagocytozed and delivered to the lysosomes (Daems et al. 1969; Steinman et al. 1983). This experiment was performed for two purposes: we wished to see (a) whether the severely vacuolated cells in the spongiosa had phagocytic activity as described for the histiocytes naturally occurring in the spongiosa layer of cardiac valves (Pfuhl 1929), and (b) whether the abnormal cytoplasmic vacuoles in histiocytes were able to fuse with endocytic vesicles.

Light microscopic staining with Turnbull's blue showed that the cellular distribution of phagocytozed iron throughout the valves was similar in the control and in the treated rat; the tracer was found only in cells of the spongiosa (Fig. 6a) and in a few endothelial cells, while the fibrosa cells were free of tracer. Ultrastructurally (Fig. 6b), the tracer was found in the histiocytes; it was contained in tilorone-induced clear vacuoles, where it was embedded in the electron-dense matrix adherent to the limiting membrane (Fig. 6c). This indicates that the vacuoles were functional parts of the lysosomal apparatus.

5. Substrate histochemistry

(a) Staining with cationic dyes. Whole mounts of cusps from subchronically treated rats were incubated with toluidine blue (pH 2 or pH 5) and showed abnormal subepithelial cells which contained metachromatic (purple) granules and vacuoles with metachromatic halos. The same type of purple me-

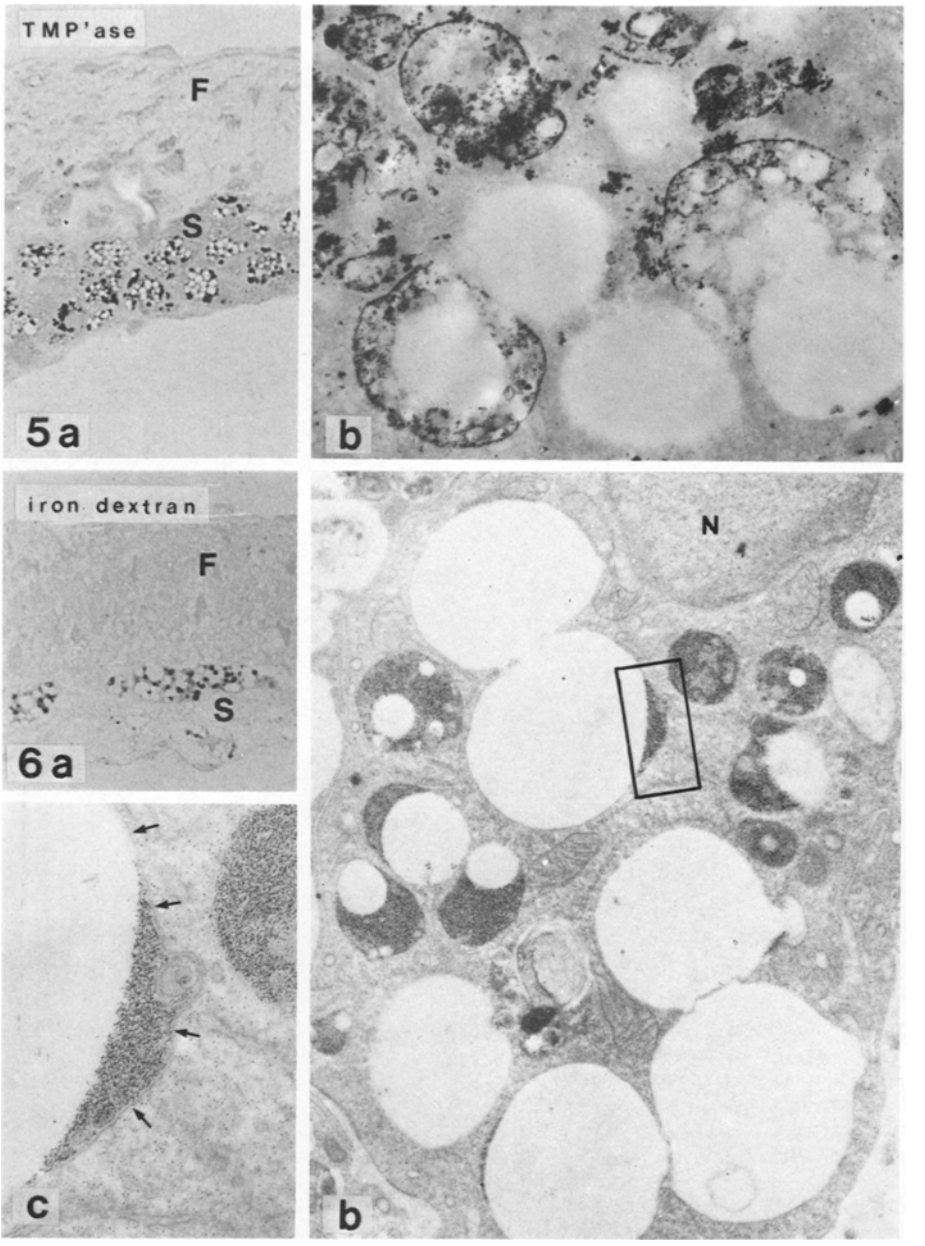

Fig. 5a, b. Demonstration of trimetaphosphatase in an aortic cusp of a rat treated with tilorone (3 wk, 80 mg/kg p.o.). **a** Unstained semithin section. The reaction product is seen in the swollen vacuolated histiocytes of the spongiosa. × 560. **b** Electron micrograph of the same preparation as in **a**. Reaction product is seen in the vacuoles of a histiocyte. Unstained section. × 25,000. For abbreviations, see legend to Fig. 1

Fig. 6a–c. Aortic cusp of a rat treated with tilorone (21 wk, 60 mg/kg p.o.). Iron dextran was injected i.v. 24 h before tissue fixation. **a** Semithin section, Turnbull's blue stain. Iron is seen in vacuolated cells of the spongiosa. × 560. **b, c** Histiocyte from the spongiosa. The tracer is found in tilorone-induced vacuoles, where it is embedded in the electron-dense matrix adherent to the limiting membrane (*arrows* in **c**). Unstained section. **b**, × 13,200; **c**, × 40,000. For abbreviations, see legend to Fig. 1

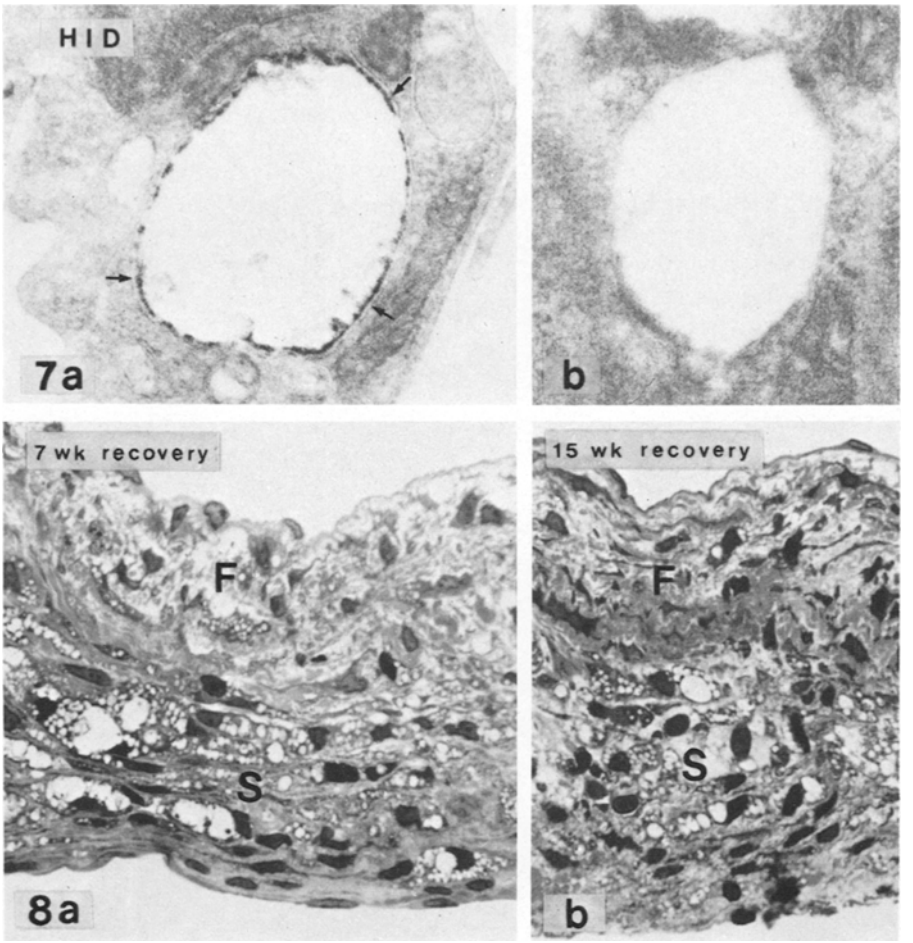

Fig. 7. a Vacuole in a histiocyte in the aortic valve of a rat treated with tilorone (13 wk, 85 mg/kg p.o.). High iron diamine procedure (HID) for demonstration of polyanionic material in the vacuoles. Unstained section. Positive staining is seen at the periphery of the vacuole (*arrows*). ×40,000. **b** Vacuole in a histiocyte from a control preparation incubated in a medium containing $MgCl_2$ instead of $FeCl_3$. No staining is obtained. ×40,000. For abbreviations, see legend to Fig. 1

Fig. 8a, b. Aortic cusps of rats treated with tilorone (13 wk, 80 mg/kg p.o.) and thereafter left without drug treatment for 7 weeks **a** and 15 weeks **b**, respectively. **a** The spongiosa is still crowded with vacuolated cells; fibroblasts of the fibrosa also show clear vacuoles. ×640. **b** The spongiosa resembles that in **a**, whereas in the fibrosa less vacuolated cells are seen. **a**, **b**, semithin sections, toluidine blue-pyronin, ×640. For abbreviations, see legend to Fig. 1

tachromasia was seen in mast cells which were regularly present in whole mounts. By focussing, the vacuolated cells were seen to belong to the spongiosa layer. After incubation with Alcian blue the same type of vacuolated cells was stained; the staining results were positive in the presence of $MgCl_2$ concentrations up to 0.5 M, while staining was abolished by 0.7 M $MgCl_2$.

The same "critical electrolyte concentration" (Scott and Dorling 1965) was found for cartilagineous matrix which was included as reference in all Alcian blue experiments, whereas mast cells were stained even at $MgCl_2$ concentrations beyond 1.0 M.

(b) High iron diamine method (HID). The procedure of Spicer et al. (1978) for the ultrastructural demonstration of sulphated polyanionic material yielded electron-dense precipitates which were located at the periphery of the otherwise empty vacuoles (Fig. 7); in specimens incubated in the control medium such precipitates were entirely absent.

6. Recovery experiments

After discontinuation of drug treatment the cytoplasmic vacuoles persisted for many weeks: 2 and 4 weeks after the end of subchronic treatment (6 wk), and 7 weeks (Fig. 8a) after chronic treatment (13 wk) the alterations of both heart valves were similar as in corresponding animals which had been sacrificed immediately at the end of treatment. After 15 weeks of recovery from chronic treatment (Fig. 8b) the fibrosa layer contained only a few vacuolated cells, whereas in the spongiosa layer many vacuolated cells, most of them histiocytes, were still present. In the connective tissue of the cardiac skeleton, vacuolation persisted for similarly long periods, whereas in atrial and ventricular walls the alterations in connective tissue cells had largely disappeared after 15 weeks of recovery.

Discussion

The present study shows that the cardiac valves of rats are markedly affected by the tilorone-induced storage disorder. The cytological alterations were most prominent in the histiocytes and fibroblasts of the spongiosa layer. According to their ultrastructural appearance and histochemical features, the vacuoles closely resembled the tilorone-induced vacuoles in hepatic and splenic sinus endothelia (Lüllmann-Rauch 1982, 1983). On the basis of the present histochemical results, the vacuoles are interpreted to be due to lysosomal storage of polyanionic material, most probably of acid glycosaminoglycans (aGAG). The critical $MgCl_2$ concentration (>0.5 M) necessary to abolish staining with Alcian blue shows that the degree of acidity of the storage material in cells of the spongiosa layer was similar to that of aGAG in cartilagineous matrix. The same was previously found for the storage material in hepatic sinusoidal wall cells (Lüllmann-Rauch 1983). The significance of the polymorphous inclusions and degenerative alterations seen in fibroblasts, but never in histiocytes, of chronically treated rats remains unclear at present. Fibroblasts at other sites in the heart or in other organs did not show such degeneration.

The alterations in valves of tilorone-treated rats show structural similarities with the changes in cardiac valves of humans and animals with inherited mucopolysaccharidoses. Such valves were reported to be thickened, and

their stroma was crowded with vacuolated cells (Okada et al. 1967; Renteria et al. 1976; Haskins et al. 1980, 1983; Shull et al. 1984), which contained metachromatically staining storage material, provided the fixation procedure was appropriate to preserve it (Lagunoff et al. 1962; Wolfe et al. 1964; Lagunoff and Gritzka 1966).

The origin of the vacuolated cells in human heart valves has not been clearly identified (Lagunoff and Gritzka 1966; Renteria and Ferrans 1976). Obviously, human valves are examined only in advanced stages of the storage disease, when the histological architecture of the valvular leaflets is greatly distorted. The present study shows that at least in tilorone-induced mucopolysaccharidosis both cell types which naturally reside in the spongiosa layer contribute to the population of vacuolated cells, with histiocytes being more susceptible than fibroblasts. The fibroblasts of the fibrosa layer were the least susceptible cells. Under the assumption that the tilorone-induced storage is due to impaired lysosomal degradation of aGAG (Lüllmann-Rauch 1983), the present findings suggest significant differences between the stromal cells with respect to their participation in the catabolism of aGAG. The observation that the cells of the spongiosa were affected earlier and more severely than those of the fibrosa, might be related to the fact that the extracellular matrix of the spongiosa layer is particularly rich in aGAG (Tretjakoff 1928; Gross 1961; Murata 1981; Mori and Honda 1982).

Concerning the pathophysiological consequences, the severe alterations in inherited human mucopolysaccharidoses often lead to valvular stenosis or regurgitation (Spranger 1972). It would be interesting to know whether such functional alterations occur also in the cardiac valves of tilorone-treated rats and might be used as a model in investigative cardiology.

Acknowledgements. The authors wish to thank Dagmar Niemeier for excellent technical assistance throughout this study, and Heide Siebke and Heidi Waluk for the photographical work.

References

Albertini A v (1953) Zur Pathogenese des rheumatischen Granuloms. Schweiz Med Wochenschr 83:772–776

Daems WT, Wisse E, Brederoo P (1969) Electron microscopy of the vacuolar apparatus. In: Dingle JT, Fell HB (eds). Lysosomes in biology and pathology, vol 1. North-Holland, Amsterdam, pp 64–112

Doty SB, Smith CE, Hand AR, Oliver C (1977) Inorganic trimetaphosphatase as a histochemical marker for lysosomes in light and electron microscopy. J Histochem Cytochem 25:1381–1384

Gross TJ (1961) Über den histologischen Aufbau der Herzklappen des Meerschweinchens. Pathol Microbiol 24:397–408

Gross L, Kugel MA (1931) Topographic anatomy and histology of the valves in the human heart. Am J Pathol 7:445–473

Haskins ME, Aguirre GD, Jezyk PF, Patterson DF (1980) The pathology of the feline model of mucopolysaccharidosis VI. Am J Pathol 101:657–674

Haskins E, Aguirre GD, Jezyk PF, Desnick RJ, Patterson DF (1983) The pathology of the feline model of mucopolysaccharidosis I. Am J Pathol 112:27–36

Ito S, Winchester RJ (1963) The fine structure of the gastric mucosa in the bat. J Cell Biol 16:541–577

Kühnel W (1966) Elektronenmikroskopische Untersuchungen über den unterschiedlichen Bau der Herzklappen. I. Mitralis und Aortenklappe. Z Zellforsch 69:452–473

Lagunoff D, Gritzka TL (1966) The site of mucopolysaccharide accumulation in Hurler's syndrome. Lab Invest 15:1578–1588

Lagunoff D, Ross R, Benditt EP (1962) Histochemical and electron microscopic study in a case of Hurler's disease. Am J Pathol 41:273–286

Lüllmann-Rauch R (1982) Histochemical evidence for lysosomal storage of acid glycosaminoglycans in splenic cells of rats treated with tilorone. Histochemistry 76:71–87

Lüllmann-Rauch R (1983) Tilorone-induced lysosomal storage mimicking the features of mucopolysaccharidosis and of lipidosis in rat liver. Virchows Arch [Cell Pathol] 44:355–368

Mori Y, Honda A (1982) Glycosaminoglycans and proteoglycans of cardiac tissue: with special reference to cardiac valves. In: Varma RS, Varma R (eds) Glycosaminoglycans and proteoglycans in physiological and pathological processes of body systems. Karger, Basel, pp 187–198

Murata K (1981) Acidic glycosaminoglycans in human heart valves. J Mol Cell Cardiol 13:281–292

Okada R, Rosenthal IM, Scaravelli G, Lev M (1967) A histopathologic study of the heart in gargoylism. Arch Pathol 84:20–30

Pfuhl W (1929) Die Histiozyten der Herzklappen, ihre Form und ihr Verhalten gegen Vitalfarbstoffe und verschiedene Reizstoffe. Z Mikr Anat Forsch 17:1–40

Regelson W (1981) The biological activity of the synthetic polyanion, pyran copolymer (diveema, MVE 46015) and the heterocyclic bis DEAE fluorenone derivative, tilorone and congeners: clinical and laboratory effect of these agents as modulators of host resistance. Pharmacol Ther 15:1–44

Renteria VG, Ferrans VJ (1976) Intracellular collagen fibrils in cardiac valves of patients with the Hurler syndrome. Lab Invest 34:263–272

Renteria VG, Ferrans VJ, Roberts WC (1976) The heart in the Hurler syndrome. Am J Cardiol 38:487–501

Scott JE, Dorling J (1965) Differential staining of acid glycosaminoglycans (mucopolysaccharides) by Alcian blue in salt solutions. Histochemie 5:221–233

Shull RM, Helman RG, Spellacy E, Constantopoulos G, Munger RJ, Neufeld EF (1984) Morphologic and biochemical studies of canine mucopolysaccharidosis I. Am J Pathol 114:487–495

Spicer SS, Hardin JH, Setser ME (1978) Ultrastructural visualization of sulphated complex carbohydrates in blood and epithelial cells with the high iron diamine procedure. Histochem J 10:435–452

Spranger J (1972) The systemic mucopolysaccharidoses. Erg Inn Med Kinderheilk [Neue Folge] 32:165–265

Steinman RM, Mellman IS, Muller WA, Cohn ZA (1983) Endocytosis and the recycling of plasma membrane. J Cell Biol 96:1–27

Tretjakoff D (1928) Das basophile Gallertgewebe. Z Mikr Anat Forsch 12:30–60

Van Hoof F (1973) Mucopolysaccharidoses. In: Hers GH, Van Hoof F (eds) Lysosomes and storage diseases. Academic Press, New York, pp 217–259

Wolfe HJ, Blennerhasset JB, Young GF, Cohen RB (1964) A histochemical study. New techniques for localization of very water-soluble acid mucopolysaccharides. Am J Pathol 45:1007–1027

Received August 6 / Accepted September 7, 1984